Supraventricular Tachycardia Classification in the 12-Lead ECG Using Atrial Waves Detection and a Clinically Based Tree Scheme

Or Perlman, Amos Katz, Guy Amit, and Yaniv Zigel, *Member, IEEE*

***Abstract*—Specific supraventricular tachycardia (SVT) classification using surface ECG is considered a challenging task, since the atrial electrical activity (AEA) waves, which are a crucial element for obtaining diagnosis, are frequently hidden. In this paper, we present a fully automated SVT classification method that embeds our recently developed hidden AEA detector in a clinically based tree scheme. The process begins with initial noise removal and QRS detection. Then, ventricular features are extracted. According to these features, an initial AEA-wave search window is defined and a single AEA-wave is detected. Using a synthetic Gaussian signal and a linear combination of 12-lead ECG signals, all AEA-waves are detected. In accord with the atrial and ventricular information found, classification to atrial fibrillation, atrial flutter, atrioventricular nodal reentry tachycardia, atrioventricular reentry tachycardia, or sinus rhythm is performed in the framework of a clinically oriented decision tree. A study was performed to evaluate the classification from 68 patients (26 were used for the classifier's design, 42 were used for its validation). Average sensitivity of 83.21% [95% confidence interval (CI): 79.33–86.49%], average specificity of 95.80% (95% CI: 94.73–96.67%), and average accuracy of 93.29% (95% CI: 92.13–94.28%) were achieved compared to the definite diagnosis. In conclusion, the presented method may serve as a valuable decision support tool, allowing accurate detection of SVTs using noninvasive means.**

***Index Terms*—Atrial electrical activity, cardiac arrhythmia classification, electrocardiogram, supraventricular tachycardia.**

I. Introduction

CARDIAC tachyarrhythmias can be roughly divided according to their anatomical origin into ventricular tachycardias (VTs), originating in the ventricles, and supraventricular tachycardias (SVTs), originating above the ventricles [1]. Since the atrial electrical activity (AEA) waves (commonly referred to as P waves), that are a significant factor in arrhythmia (including SVT) classification, are sometimes concealed in other electrocardiogram (ECG) waves, accurate arrhythmia diagnosis is seldom available without invasive electrophysiology study (EPS) [2]. The case-specific arrhythmia diagnosis is clinically important and involves clinical implications. Accurate diagnosis of the SVT mechanism relies on the relationship between the ventricular electrical activity and the AEA.

Various algorithms were developed in order to detect and diagnose SVTs. Several studies proposed arrhythmia classification using the heart rate signal [3]–[5]. In this approach, parameters derived from the QRS detection serve as input to a neural network [3], a support vector machine [4], or a knowledge-based method [5] in order to distinguish several arrhythmias. However, the only SVT class included in this approach is atrial fibrillation (AF). In a different method [6], bispectral analysis technique, which classifies normal sinus rhythm, VT, VF, and AF, was used. Good results were demonstrated using a prony modeling algorithm [7], which classified VF, VT, and a general group of SVTs. To conclude, existing arrhythmia classification algorithms usually regard SVT as a separate global class, without specifically indicating the exact arrhythmia [8], or include classification to a single SVT case.

Development of an arrhythmia classification algorithm that is able to diagnose and separate specific types of SVT using a 12-lead ECG may guide the cardiologist/cardiac electrophysiologist in how to treat the patient and whether to use the invasive EPS and ablation pathway or to try medical therapy. If an EPS is indeed required, the result of the SVT classification algorithm will allow improved planning beforehand and provide optimal treatment to the patient.

The aim of this study is to propose a fully automated computerized algorithm for classifying the five following cases using 12-lead ECG signals: AF, atrial flutter, atrioventricular nodal reentry tachycardia (AVNRT), atrioventricular reentry tachycardia (AVRT), and sinus rhythm. Some preliminary results of our study were presented in [9]. This paper contains a further significant development, a more thorough analysis, and more complete results.

II. Methods

The proposed algorithm is based on combining both AEA and ventricular electrical activity related information in a clinically oriented set of rules (tree scheme) aimed to detect and distinguish SVTs. The method is composed of the following stages (see Fig. 1):

A. Noise Removal

An eight-order bandpass Butterworth forward/backward filter with cutoff frequencies of 0.5 and 49.5 Hz is being used in all 12

Manuscript received June 17, 2015; revised August 13, 2015; accepted September 6, 2015. Date of publication September 23, 2015; date of current version December 6, 2016. *(Corresponding author: Yaniv Zigel.)*

O. Perlman and Y. Zigel are with the Department of Biomedical Engineering, Faculty of Engineering, Ben-Gurion University of the Negev, Beer-Sheva 84105, Israel (e-mail: perlmano@post.bgu.ac.il; yaniv@bgu.ac.il).

A. Katz is with the Faculty of Health Sciences, Ben-Gurion University of the Negev, Beer-Sheva 84105, Israel, and also with the Barzilai Medical Center, Ashkelon 78278, Israel (e-mail: amoskatz@bgu.ac.il).

G. Amit is with the Faculty of Health Sciences, Ben-Gurion University of the Negev, Beer-Sheva 84105, Israel, and also with the Soroka University Medical Center, Beer-Sheva 84105, Israel (e-mail: guyamit@bgu.ac.il).

Color versions of one or more of the figures in this paper are available online at http://ieeexplore.ieee.org.

Digital Object Identifier 10.1109/JBHI.2015.2478076

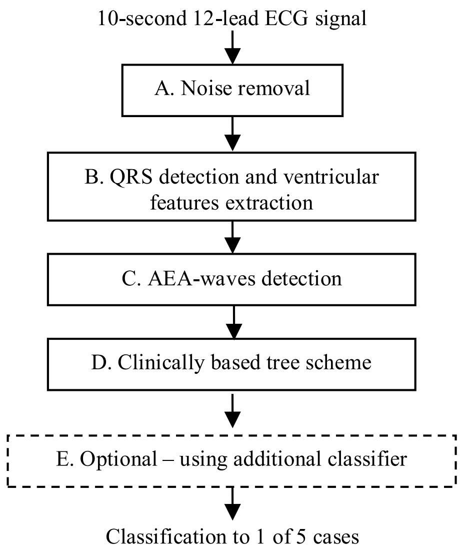

Fig. 1. Block diagram of the method's stages.

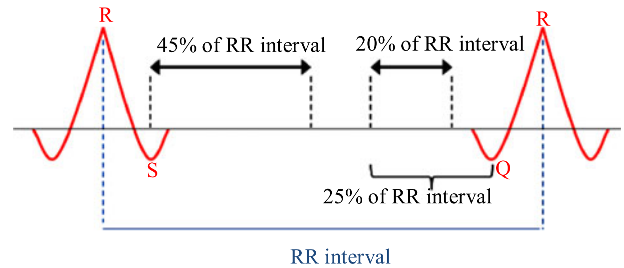

Fig. 2. Two possible search windows for initial AEA-wave detection. The before-QRS-window starts 25% of the mean RR-interval before the Q-wave and ends 20% of the RR-interval later. The after-QRS-window starts at the S-wave and ends 45% of the mean RR-interval later.

leads, to avoid common ECG noises (power-line noise, baseline wander, etc.) and to retain the AEA-waves, whose energy is mostly limited to less than 49 Hz.

B. QRS Detection and Ventricular Features Extraction

The signal's QRS complexes are found using a well-known commonly used method [10] and the heart rate (in beats/min units) is calculated. Next, the time intervals between subsequent R waves (RR-intervals) are calculated and a measure representing the ventricular regularity is obtained by dividing the RR-interval standard deviation by the RR-interval mean. The described stage is performed by default in lead II. If required by stage C2 (as will later be described), this step is reperformed using lead V1.

C. AEA-Waves Detection

Depending on the arrhythmia case, the AEA-waves may appear after the QRS, close to the previous or to the next QRS (e.g., in AVRT), simultaneous or immediately after the QRS (e.g., in AVNRT), be visually discernible (e.g., in sinus rhythm) or concealed in other ECG waves (e.g., AEA-wave concealed inside a T wave during atrial flutter) [11]. A recently developed AEA-detection method demonstrated an impressive ability in detecting AEA-waves during various arrhythmias, even when they are concealed [2]. However, this novel detector is semi-automatic, and requires the initial manual segmentation of one AEA-wave. As part of this paper, we suggest a means for automating it. Since the AEA information is crucial for obtaining an accurate SVT diagnosis [12], embedding such an automatic AEA detector in an arrhythmia classifying algorithm may be highly beneficial. The AEA-detection procedure performed here can be divided to four steps:

1) Defining an initial AEA-wave search window for the currently evaluated signal. The window can be positioned before each QRS complex (starts a seconds before the Q wave and ends b seconds later) or after it (starts at the S wave and ends c seconds later). In order to adapt the search window to the specific input signal characteristics, the values a–c are determined respective to the mean RR interval: $a = $ (25% of the mean RR-interval length); $b = $ (20% of the mean RR-interval length); $c = $ (45% of the mean RR-interval length). These values were chosen based on empirical evaluation of the training database (see Section III). The decision of using the before-QRS-window or the after-QRS-window (see Fig. 2) is performed according to the heart rate (extracted in this section, stage *B*) and as part of a clinically based tree scheme (see this section step *D* and Fig. 3).
2) Automatic detection of a single AEA-wave. We first assume that the input signal contains at least one detectable AEA-wave that is not entirely concealed by other waves. We then automatically find the peak of that single AEA-wave [see Fig. 4(a)] by using a low-pass differentiation-based method [13] in the previously defined search window in lead II. In case a single AEA-wave was not found in lead II either before the QRS or after it, lead V1 is used (with features reextracted from step B using lead V1). In case more than one AEA-wave was found, the earliest one detected is selected for the next step.
3) Detection of all AEA-waves. At this step, we exploit our recently developed method for detecting AEA-waves [2]. This method gets one AEA wave as input (defined as 40 ms before and after the AEA-wave's peak—in our case the one found at the previous step). According to this single AEA-wave, a synthetic Gaussian signal is created (denoted as $g[k]$) [see Fig. 4(b)]. Next, the linear combination of eight ECG leads (I, II, $V1, V2, V3, V4, V5$, and $V6$—with a corresponding matrix denoted as $\mathbf{l}[k]$) is constrained to be as similar as possible to the Gaussian signal in the minimum mean square error sense, therefore creating an output signal $\tilde{a}[k]$ with emphasized AEA [14]:

$$\tilde{a}[k] = \mathbf{w}^T \mathbf{l}[k] \tag{1}$$

where $\mathbf{w}$ is the weight coefficients vector. The suitable weight vector is obtained using

$$\mathbf{w} = \mathbf{R}^{-1}\mathbf{r} \tag{2}$$

where $\mathbf{R}$ is the correlation matrix of the eight ECG leads

$$\mathbf{R}[k] = E[\mathbf{l}[k]\mathbf{l}[k]^T] \tag{3}$$

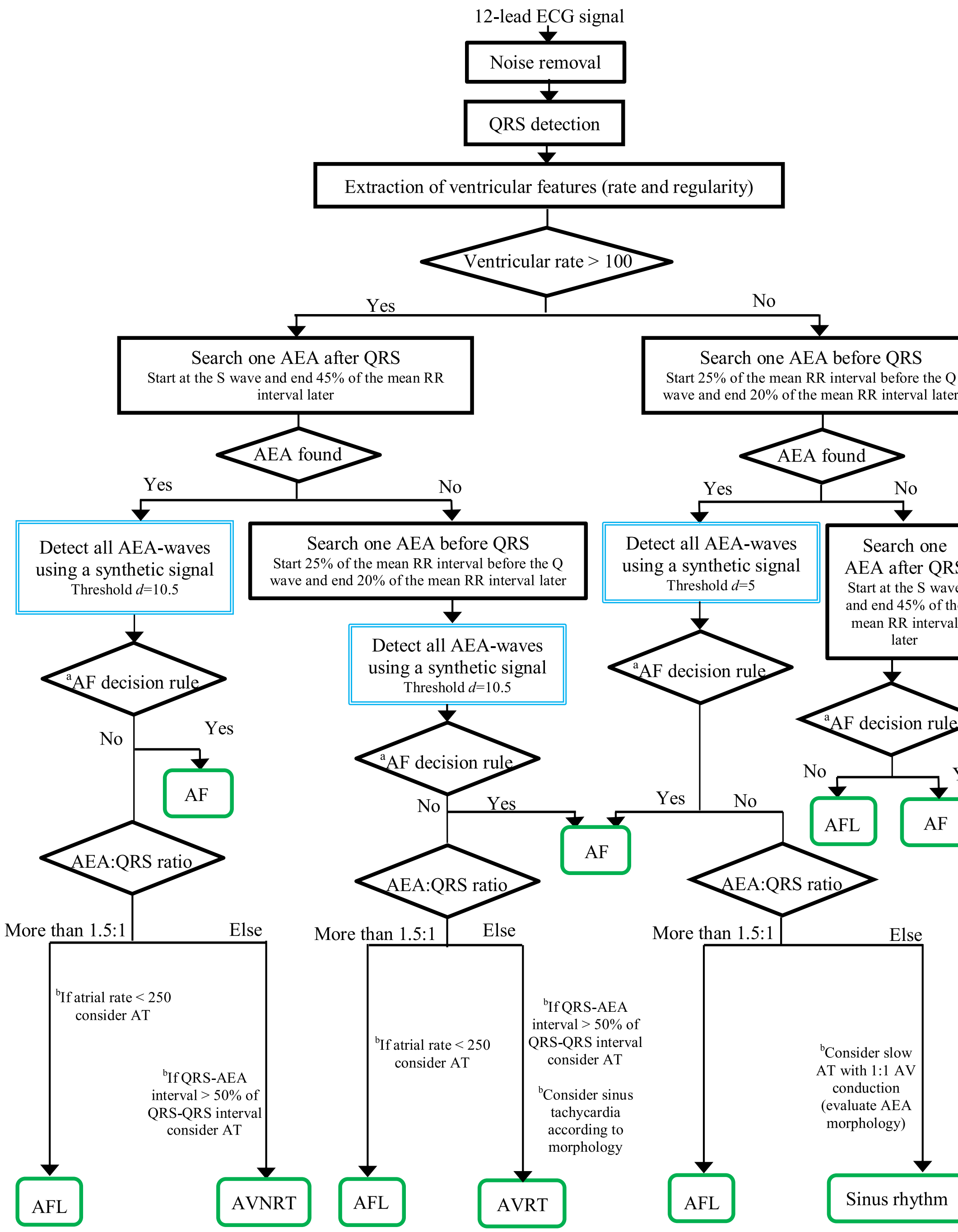

Fig. 3. Clinically based tree scheme. The flowchart leads to a final classification of five possible cases (green rounded blocks), using the AEA detection method that uses synthetic atrial activity signal (blue double-framed blocks). [a]The AF decision rule is described in the text—Section II-D. [b]Although AT and sinus tachycardia cannot definitely be diagnosed using the described algorithm, for completeness of information considerations, the algorithm enables letting the user acknowledge the cases in which these arrhythmias should be considered. AVRT = atrioventricular reentry tachycardia, AVNRT = atrioventricular nodal reentry tachycardia, AFL = atrial flutter, AT = atrial tachycardia, AF = atrial fibrillation.

and $\mathbf{r}$ is the cross-correlation vector of the eight ECG leads and the synthetic Gaussian signal

$$\mathbf{r}[k] = E[g[k]\mathbf{1}[k]]. \tag{4}$$

The output signal $\tilde{a}[k]$ contains peaks only at the locations corresponding to the actual AEA-wave locations [see Fig. 4(c)]. After additional 2–16 Hz bandpass filtering, the peaks in this emphasized AEA signal [see Fig. 4(d)] that are higher than a certain threshold are determined as AEA-waves (the threshold is determined as the top $d\%$ value of the peaks' amplitudes in the filtered emphasized AEA signal). Since various arrhythmias may require different thresholds, in this study, the threshold (d) is determined as part of a clinically based tree scheme (see step D and Fig. 3).

4) Although the AEA detector used in the former step is satisfyingly accurate [2], it may result in some exceptional cases of AEA-wave false detection inside the QRS

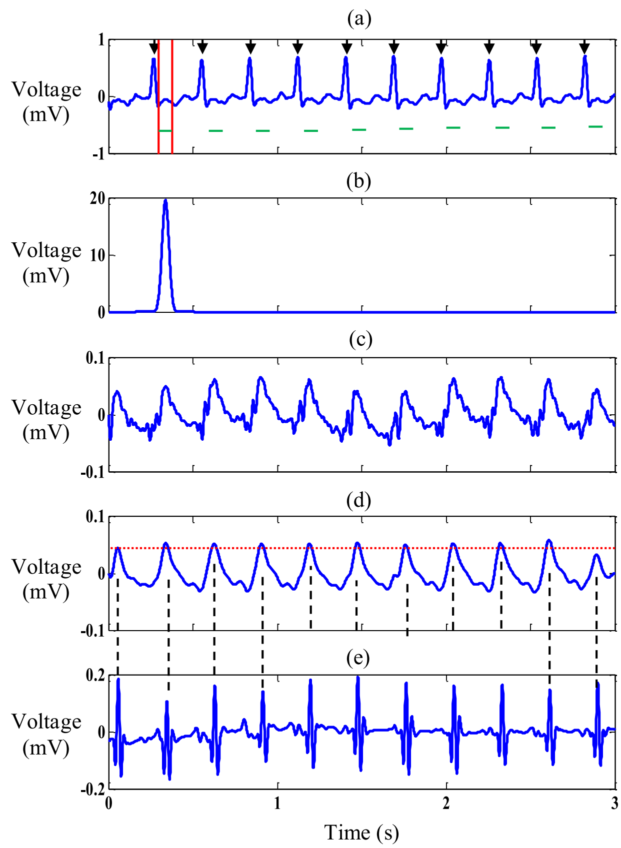

Fig. 4. Example of the clinically based tree scheme classification procedure. From top to bottom: (a) A signal containing AVNRT (lead II) after noise removal. The arrows mark the detected QRS complexes, from which the heart rate is calculated (200 bpm). According to the over-100 heart rate, a single AEA-wave search window after the QRS complex is used [horizontal lines (green)]. The earliest AEA-wave detected [vertical lines (red)] is used as input to the method aimed for detection of all AEA-waves. (b) According to the AEA detection method, a synthetic signal is created and used to obtain an emphasized AEA signal. (c) The resulting emphasized AEA signal. (d) Bandpass-filtered emphasized AEA signal. The peaks in this signal higher than a threshold determined by the tree scheme [horizontal line (red)] are determined as AEA-waves. (e) Intraatrial electrode signal, used only for performance evaluation. The peaks in this signal correspond to the actual AEA-waves. The vertical lines indicate that the resulting higher-than-threshold peaks, in the bandpassed emphasized AEA signal, match the true AEA-wave locations in all cases except the last AEA-wave. Since 10 QRS complexes and 10 AEA-waves were detected by the described procedure, the AEA:QRS ratio is 1:1. The signal fails to qualify the AF decision rule (due to its evident ventricular regularity) and is, therefore, successfully classified by the decision tree as AVNRT.(a) AVNRT (lead II) (b) Synthetic AEA signal (c) Resulting emphasized AEA signal (d) Filtered emphasized AEA signal (e) Intraatrial electrode signal.

complex. In this step, we reject any AEA-waves detected between the Q and S waves.

D. Clinically Based Tree Scheme

During stages *A–C* both ventricular electrical activity and AEA related information were extracted. In order to conclusively determine if an SVT is present in the input signal, and if so to classify the exact one, a clinically based tree scheme, which integrates all gathered information, is used. The scheme was devised by careful scrutiny of clinical ECG characteristics of various SVTs, derived from well-established cardiology literature sources and recognized guidelines for discrimination [12], [15], [16]. Several parameters were slightly adapted according to the training database evaluation (see Section III) with the guidance and supervision of expert cardiac electrophysiologists. The concept of this scheme is to mimic the physician's arrhythmia diagnosis procedure. As described in the previous step, an additional role of this scheme is to determine the adequate AEA detection search window and parameters used, according to the different cases. For example, if the scheme reached a decision point between sinus rhythm and atrial flutter, a threshold of $d = 5$ will be used in the AEA-detection step, since it is mostly suitable to distinguish these two cases [2]; whereas in case the scheme reached a decision point between AVNRT and atrial flutter, a threshold of $d = 10.5$ will be used.

A special case in the classification tree is AF. This arrhythmia is characterized by irregular ventricular rate and atrial activity [15], [17]. The mechanism is fast firing foci or atrial reentrant circuits [18]. Therefore, it is suggested here to use the following decision rule, in which three conditions must be fulfilled in order for the signal to be classified as AF:

1) The ventricular activity is irregular. This is quantified by a ventricular regularity measure (see Section II-B) that is higher than 10% for AF (a similar value was used in [19].
2) The atrial activity is irregular, and may be generated by multiple sources. When multiple sources contribute to the AEA, it cannot be fully extracted and assessed using a single found AEA-wave, as described in Section II, step C3 [2]. In this case, the AF-related AEA is underestimated, and only part of it is obtained, depending on the specific source initially found. However, significant utility can still rise from this information. By repeating the linear combiner method for *all* initial AEA-wave candidates found at stage C2, a representation of several possible atrial sources can be obtained. In order to decide if the AEA-emphasized signals contain a single source or several, the correlation coefficients of all resulting AEA signal combinations are calculated and averaged. A low-averaged correlation value indicates the existence of several sources (appropriate for AF), whereas a high value indicates existence of a single atrial source (appropriate for other arrhythmias or sinus rhythm). Based on the evaluation of a separate training database (see Section III-B), the correlation coefficient threshold was determined as 0.86.
3) The above described correlation coefficient measure may provoke increase in the application runtime. It can in some cases be avoided by checking the AEA:QRS ratio prior to the above described step 2. In AF signals, the linear combiner method output of a *single* found AEA wave candidate with a threshold of $d = 5\%$ tends to result in an exact or less than 1.5 AEA:QRS ratio. This is due to revealing only a *single* atrial source instead of all of them, and was verified on the training database—see Section III. Using this characteristic can increase accuracy as well as reduce the application runtime.

In summary, the AF decision rule comprises three subsequently checked conditions that must all be fulfilled: ventricular regularity higher than 10%, AEA:QRS ratio equal to or smaller than 1.5, and average correlation smaller than 0.86.

The clinically based tree scheme can be seen in Fig. 3. An example of the clinically based tree scheme classification procedure can be seen in Fig. 4.

E. Optional—Using an Additional Two-Class Classifier

Although the use of the clinically based tree scheme resulted in correct classification and satisfying performance in most cases, in some extreme cases the final decision is mistaken (as will later be demonstrated—see Section IV-A). The original challenging problem of classifying five classes (AF, atrial flutter, AVNRT, AVRT, and sinus rhythm) is significantly simplified by using the tree scheme, which eventually concludes in distinguishing two classes. For example, in the left-most branch of the scheme (see Fig. 3), the classification is narrowed to atrial flutter and AVNRT and then a single class is determined. The final mistakes are mainly related to specific two-class confusions—mainly falsely detecting AVNRT as AVRT and vice versa (see Section IV-A). In order to further improve performance, a simple optional solution is suggested: whenever the tree scheme results in classifying AVNRT or AVRT, the input signal will undergo another simple classification procedure, aimed to verify that confusion between the two classes did not occur. The 5-nearest-neighbors (5-NN) classifier was found to be adequate [20]. According to this classifier, each input signal is related to a feature vector, represented in a multidimensional space. In our case a 4-D space was found suitable, with the use of two RR-interval related features (based on the energy of the RR-intervals signal, calculated using short time Fourier transform [21]), the AEA:QRS ratio with the adaptive threshold suggested in [2], and the AEA position (where 0-value denotes AEA before QRS and 1-value denotes AEA after QRS). The above-listed features can be found easily using the information gathered during the tree scheme steps, and are calculated for each signal of the training database as well as the input (validation) signal. Finally, this classifier assigns to the input signal, the classification of the majority between the nearest five training feature vectors [22]. In brief, the final classification of AVNRT or AVRT will be performed by comparing the described characteristics of the currently evaluated validation signal with the characteristics of the training database signals. According to the majority class (AVNRT/AVRT) of the most "similar" five training database signal characteristics to the input signal characteristics, the decision is made.

III. Experimental Setup

A. Subjects

We prospectively and consecutively included 66 patients who were directed to one of two medical centers—Barzilai Medical Center, Ashkelon, Israel, or Soroka Medical Center, Beer-Sheva, Israel, for an EPS. The patients' hearts were normal without any structural abnormalities, without clinical or angiographic evidence of coronary artery disease. The left ventricular ejection fraction was normal in all the patients. Of the patients with atrial flutter, 10% had controlled hypertension (without left ventricular hypertrophy). Ethics approvals for the study were granted from each respective medical center's ethics committee. In addition, two patients' 12-lead ECG recordings from St. Petersburg Institute of Cardiological Technics' 12-lead arrhythmia database [23] were added to the study cohort. A total of 26 arbitrary patients were defined as the training set (for designing the classifier and defining its parameters) and 42 arbitrary patients were defined as the validation set (for evaluating the classifier performance). The study cohort included patients diagnosed with the following SVTs: AF, atrial flutter, AVRT, AVNRT, and sinus rhythm, after other arrhythmias were ruled out.

TABLE I
Database Properties

Database	Training		Validation	
Rhythm Case	Number of signals	Number of patients	Number of signals	Number of patients
Sinus Rhythm	86	12	99	24
Atrial flutter	91	6	108	7
AVNRT	38	6	52	12
AVRT	52	5	69	7
AF	74	3	89	6
Total	341	26[a]	417	42[b]

[a,b]Some patients presented more than one rhythm case; AF = atrial fibrillation, AVRT = atrioventricular reentry tachycardia, AVNRT = atrioventricular nodal reentry tachycardia.

B. ECG Recording

During EPS, 12-lead ECG recordings were performed as well as intraatrial ECG recordings, using GE Cardiolab IT, which produces electrograms sampled at 977 Hz with 12-bit analog-to-digital conversion. The intraatrial recordings were only used for establishing the diagnosis of the exact SVT by two expert cardiac electrophysiologists. The 12-lead surface ECG signals were consecutively divided to 10-s-long signals. Three hundred and forty one such signals from 26 random patients served as training database (including the two St. Petersburg arrhythmia database patients [23], and 417 such signals from the remaining 42 patients served as validation database. For detailed database properties see Table I.

C. Performance Measures and Statistical Analysis

In order to evaluate the performance of the SVT automatic classifier, the sensitivity:

$$\mathrm{Sensitivity} = \frac{\mathrm{TP}}{\mathrm{TP}+\mathrm{FN}}, \tag{5}$$

specificity:

$$\mathrm{Specificity} = \frac{\mathrm{TN}}{\mathrm{FP}+\mathrm{TN}}, \tag{6}$$

and accuracy measures:

$$\mathrm{Accuracy} = \frac{\mathrm{TP}+\mathrm{TN}}{\mathrm{TP}+\mathrm{TN}+\mathrm{FP}+\mathrm{FN}} \tag{7}$$

were calculated. TP, FP, TN, and FN correspond to true positive, false positive, true negative, and false negative, respectively. The measures were calculated using a multiclass confusion matrix [24], which was later divided by each class' total number of

TABLE II
PERFORMANCE ANALYSIS FOR SVT CLASSIFICATION

Validation database						
Method	*Clinically based tree scheme*			*Clinically based tree scheme with additional two-class classifier - 5NN*		
Rhythm Case	*Sensitivity (%)*	*Specificity (%)*	*Accuracy (%)*	*Sensitivity (%)*	*Specificity (%)*	*Accuracy (%)*
Sinus Rhythm	93.94 (CI: 87.40–97.19)	97.48 (CI: 95.12–98.72)	96.64 (CI: 94.44–97.99)	93.94 (CI: 87.40–97.19)	97.48 (CI: 95.12–98.72)	96.64 (CI: 94.44–97.99)
Atrial flutter	82.41 (CI: 74.15–88.44)	97.09 (CI: 94.56–98.46)	93.29 (CI: 90.47–95.31)	82.41 (CI: 74.15–88.44)	97.09 (CI: 94.56–98.46)	93.29 (CI: 90.47–95.31)
AVNRT	63.46 (CI: 49.87–75.20)	94.52 (CI: 91.69–96.43)	90.65 (CI: 87.47–93.08)	71.15 (CI: 57.73–81.67)	96.16 (CI: 93.67–97.70)	93.05 (CI: 90.19–95.11)
AVRT	73.91 (CI: 62.49–82.81)	94.54 (CI: 91.63–96.48)	91.13 (CI: 88.01–93.49)	79.71 (CI: 68.78–87.51)	95.11 (CI: 92.32–96.93)	92.57 (CI: 89.64–94.71)
Atrial fibrillation	82.02 (CI: 72.77–88.62)	93.29 (CI: 90.05–95.53)	90.89 (CI: 87.74–93.29)	82.02 (CI: 72.77–88.62)	93.29 (CI: 90.05–95.53)	90.89 (CI: 87.74–93.29)
Total	81.30 (CI: 77.27–84.75)	95.32 (CI: 94.20–96.24)	92.52 (CI: 91.31–93.57)	83.21 (CI: 79.33–86.49)	95.80 (CI: 94.73–96.67)	93.29 (CI: 92.13–94.28)

AVNRT = atrioventricular nodal reentry tachycardia, AVRT = atrioventricular reentry tachycardia, CI = 95% confidence interval.

TABLE III
CONFUSION MATRIX FOR THE PROPOSED ARRHYTHMIA CLASSIFIER (PERCENTAGE DISPLAY)

Validation database											
Method		*Clinically based tree scheme*					*Clinically based tree scheme with an additional two-class classifier (5 NN)*				
		Predicted Class									
Actual Class	***Case***	***S. R.***	***AFL***	***AVNRT***	**AVRT**	***AF***	***S. R.***	***AFL***	***AVNRT***	**AVRT**	**AF**
	S.R.	93.94	3.03	0.00	0.00	3.03	93.94	3.03	0.00	0.00	3.03
	AFL	0.93	82.41	2.78	0.93	12.96	0.93	82.41	2.78	0.93	12.96
	AVNRT	0.00	0.00	63.46	32.69	3.85	0.00	0.00	71.15	25.00	3.85
	AVRT	0.00	0.00	21.74	73.91	4.35	0.00	0.00	15.94	79.71	4.35
	AF	7.87	6.74	2.25	1.12	82.02	7.87	6.74	0.00	3.37	82.02

S.R. = sinus rhythm, AFL = atrial flutter, AVNRT = atrioventricular nodal reentry tachycardia, AVRT = atrioventricular reentry tachycardia, AF = atrial fibrillation.

signals for percentage display (see Table III). Ninety-five percent confidence intervals (CI) were calculated using standard methods for proportions [25].

D. Justification of Parameters

There are several parameters incorporated in the proposed method. As stated in Section II-D, the initial parameters were devised according to well-known clinical ECG characteristics of various SVTs. In this section, we shall justify each parameter and note if it was modified.

The ventricular rate threshold was determined according to clinical theory [15]. The AEA-wave search window length and location (parameters a, b, and c) as well as the AEA:QRS ratio were roughly determined according to the AEA-wave literature characteristics [12], [15], and slightly tuned according to the training database evaluation. The AEA detection threshold d was determined according to the comprehensive analysis provided in [2]. The AF decision rule parameters were determined according to evaluation on the training database, with guidelines stemming from known clinical characteristics of this arrhythmia [15], [17], [18]. The AF ventricular regularity threshold was also supported by a previous study [19].

The optional two-class classifier parameters (see Section II-E) were determined by performing an exhaustive search feature selection procedure [26], which included the RR-intervals' related features described in [21], the AEA:QRS ratio derived by the various thresholds described in [2], heart rate, ventricular regularity, and AEA position. The number of features was limited to four, in order to prevent overfitting [27].

IV. RESULTS

A. Arrhythmia-Dependent Results

The detailed arrhythmia-dependent results can be seen in Table II. When using the clinically based tree scheme, the best performances were demonstrated in the sinus rhythm case—sensitivity, specificity, and accuracy of 93.94%, 97.48%, and 96.64%, respectively. The worst performances were demonstrated in AVNRT (sensitivity of 63.46%, specificity of 94.52%, and accuracy of 90.65%).

By analyzing the confusion matrix of the classification (see Table III), it is noticeable that the tree classifier confused AVNRT signals mostly with AVRT and vice versa. Hence, it is reasonable to assume that adding a two-class classifier for these two cases will improve results. As expected, by adding a two-class classifier specifically aimed to distinguish AVNRT and AVRT, the sensitivity, specificity, and accuracy of both AVNRT and AVRT are improved (see Table II).

B. Global Results

The global sensitivity achieved by the clinically based tree scheme was 81.30%, the global specificity was 95.32%, and

TABLE IV
COMPARISON OF ARRHYTHMIA CLASSIFICATION ALGORITHMS

Authors	Method used	Arrhythmia classes (**SVT classes are in bold**)	Performance (%)
Acharya *et al.* [3]	Heart rate signal features in a neural network or a fuzzy classifier	S.R., PVC, **AF**, SSS, VF, heart blocks, ischemic/dilated cardiomyopathy	Acc = 80−85
Asl *et al.* [4]	Heart rate signal, generalized discriminant analysis, and support vector machine	S.R., PVC, **AF**, SSS, VF, heart blocks	Se = 95.77 Sp = 99.4 Acc = 99.16
Khadra *et al.* [6]	Bispectral analysis technique	S.R., VT, VF, and **AF**	VF: Se = 91.7; Sp = 83.3 VT: Se = 81.8; Sp = 90.9 AF: Se = 83.8; Sp = 100 S.R: Se = 100; Sp = 100
Chen [7]	Prony modeling	VT, VF, **general SVT group**	General SVT group Se = 95.24 VF Se = 96.00 VT Se = 97.78
Srinivasan *et al.* [8]	Autoregressive modeling	S.R., **PAC, general SVT group**, VT, VF, PVC	Acc = 93.2–100
Jovic *et al.* [24]	Random Forest and AdaBoosted C4.5	S.R., **PAC**, PVC, VT, VBI, heart blocks, **AF**, paced rhythm	Acc = 85.63
The proposed method	Atrial waves detection and a clinically based tree scheme, with optionally adding KNN classifier	S.R., **AF, AFL, AVRT, AVNRT**	Se = 83.21 Sp = 95.80 Acc = 93.29

SVT = supraventricular tachycardia, AF = atrial fibrillation, AVNRT = atrioventricular nodal reentry tachycardia, AVRT = atrioventricular reentry tachycardia, S.R = sinus rhythm, VF = ventricular fibrillation, PVC = premature ventricular contraction, SSS = sick sinus syndrome; Se = sensitivity, Sp = specificity, Acc = accuracy, PAC = premature atrial contraction, VBI = ventricular bigeminy, VT = ventricular tachycardia, AFL = atrial fibrillation.

the global accuracy was 92.52%. When adding the two-class classifiers to the tree scheme, the global sensitivity was improved to 83.21%, the specificity was improved to 95.80%, and the accuracy was improved to 93.29%.

C. Comparison with Existing Methods

The performances of our method were compared to several other prominent existing arrhythmia classification algorithms [3], [4], [6]–[8], [24]. The results can be seen in Table IV. It should first be noted that each algorithm is suited for different arrhythmia types. AF constitutes the most commonly addressed SVT. However, none of the comparative algorithms addresses AVNRT or AVRT as a single group. In [7] and [8], a *general* SVT group is classified, however, there is no distinction between the specific SVT types. The proposed algorithm is the only one that addresses four different SVT types and differentiates them, with performances that are in the range of those of other proposed methods. To allow additional fair comparison with existing algorithms, the proposed classifier was used for discriminating sinus rhythm and a general SVT group. The resulting sensitivity, specificity, and accuracy of detecting the SVT group were 97.48%, 93.94%, and 96.64%, respectively (the performances in detecting sinus rhythm remained the same). These results are very similar to those reported in the comparison algorithms, which classified a single general SVT case [7], [8].

D. Implementation Environment and Time Complexity

The proposed SVT classification method was implemented using Mathworks Matlab software, on an Intel Core i7-4790 3.6 GHz PC. The time required for processing and classifying each 10-s-signal was approximately 131 ms using the clinically based tree scheme and approximately 137 ms using the clinically based tree scheme with an additional two-class classifier (5-NN).

V. DISCUSSION

The described SVT classifier demonstrated satisfactory performance. This is apparently rooted in the incorporation of the crucial AEA-related information in a clinically based scheme; the classifier was designed to mimic the cardiac electrophysiologist's diagnostic procedure, by using a set of rules applied on information that was aimed to approximate the gold-standard invasive electrodes rooted information. To the best of our knowledge, this is the first time a fully automated algorithm for distinguishing *various* SVTs is presented. Although some algorithms classify a general SVT group [7], [8], a great benefit may result from exact detection of the specific arrhythmia [28], such as administration of the most suitable treatment to the patient and optimal planning of the EPS.

The worst results were demonstrated in the AVNRT and AVRT cases, probably due to their highly similar signal characteristics (regular ventricular activity, heart rate ranging usually between 150 and 250 beats/min, etc. [15]). Moreover, each of these arrhythmias has several variations (slow-fast/fast-slow AVNRT, orthodromic/antidromic AVRT), which render them harder to detect and differentiate. However, a significant improvement in classifying these two classes was achieved when an additional two-class ad hoc classifier was added.

Since sinus tachycardia is not a pathologic arrhythmia (aside from rare cases [29]), and since it is easily recognizable by a physician from 12-lead ECG, it was not included in the algorithm.

AF is the most common pathologic SVT [17]. It has been the focus of various research efforts and may be detected by several existing algorithms (see Table IV and [30]). However, in most cases, other SVT cases are not included in the AF detector evaluation. As the differentiation between atrial flutter and AF is very important and holds clinical implications, the study described here holds a significant added value—classifying AF in a cohort containing three other SVT classes (including atrial flutter), as well as sinus rhythm.

The atrial wave detection method used here attempts to find a linear combination of eight ECG leads that will yield a signal that greatly resembles the actual atrial signal. Using fewer than eight leads will not exploit the entire attainable information, which may be essential for this effort [2]. For example, when using just leads I, II, and V1 (without the additional two-class classifier) the average sensitivity is reduced to 74%.

QRS detection is an essential step in the algorithm. However, since the Pan–Tompkins QRS detection method [10] is well validated and has more than 99% correct detection, it is considered highly reliable. Moreover, any other published QRS detection method can be incorporated in the proposed algorithm.

VI. Conclusion and Future Work

In spite of atrial tachycardia being less common than the rhythm cases addressed in this study, a future study should include incorporating it in the described classifier. This is a nontrivial task, since in some cases AT characteristics are very similar to those of AVNRT and AVRT. Moreover, even existing well-known diagnostic schemes [16] that provide medical care or drug administration as an additional tool for diagnosis, are only able to classify a single general group of three arrhythmias (such as AVRT, AVNRT, and AT) instead of AT solely, in some conditions. Although AT is not fully classified in the proposed method, the decision tree notifies the user of cases in which the analyzed signal may contain this arrhythmia (see the footnote in Fig. 3).

The high accuracy of the algorithm along with its relatively short runtime indicates its potential. The algorithm constitutes a substantial step toward providing a decision support system that could greatly assist emergency departments, ambulances, and monitored patients, along with implementation in commercial 12-lead ECG devices.

References

[1] J. L. Rojo-Alvarez, A. Arenal-Maiz, and A. Artes- Rodriguez, “Discriminating between supraventricular and ventricular tachycardias from EGM onset analysis,” *IEEE Eng. Med. Biol. Mag.*, vol. 21, no. 1, pp. 16–26, Jan./Feb. 2002.

[2] O. Perlman, A. Katz, N. Weissman, G. Amit, and Y. Zigel, “Atrial electrical activity detection using linear combination of 12-lead ECG signals,” *IEEE Trans. Biomed. Eng.*, vol. 61, no. 4, pp. 1034–1043, Apr. 2014.

[3] R. Acharya, A. Kumar, P. Bhat, C. Lim, N. Kannathal, and S. Krishnan, “Classification of cardiac abnormalities using heart rate signals,” *Med. Biol. Eng. Comput.*, vol. 42, no. 3, pp. 288–293, 2004.

[4] B. M. Asl, S. K. Setarehdan, and M. Mohebbi, “Support vector machine-based arrhythmia classification using reduced features of heart rate variability signal,” *Artif. Intell. Med.*, vol. 44, no. 1, pp. 51–64, 2008.

[5] M. G. Tsipouras, D. I. Fotiadis, and D. Sideris, “An arrhythmia classification system based on the RR-interval signal,” *Artif. Intell. Med.*, vol. 33, no. 3, pp. 237–250, 2005.

[6] L. Khadra, A. S. Al-Fahoum, and S. Binajjaj, “A quantitative analysis approach for cardiac arrhythmia classification using higher order spectral techniques,” *IEEE Trans. Biomed. Eng.*, vol. 52, no. 1, pp. 1840–1845, Nov. 2005.

[7] S. W. Chen, “A two-stage discrimination of cardiac arrhythmias using a total least squares-based Prony modeling algorithm,” *IEEE Trans. Biomed. Eng.*, vol. 47, no. 10, pp. 1317–1327, Oct. 2000.

[8] D. Ge, N. Srinivasan, and S. Krishnan, “Cardiac arrhythmia classification using autoregressive modeling,” *Biomed. Eng. Online*, vol. 1, pp. 1–12, 2002.

[9] O. Perlman, Y. Zigel, G. Amit, and A. Katz, “Cardiac arrhythmia classification in 12-lead ECG using synthetic atrial activity signal,” in *Proc. IEEE 27th Conv. Electr. Electron. Eng.*, Eilat, Israel, 2012, pp. 1–4.

[10] J. Pan and W. J. Tompkins, “A real-time QRS detection algorithm,” *IEEE Trans. Biomed. Eng.*, vol. BME-32, no. 3, pp. 230–6, Mar. 1985.

[11] D. Goldwasser *et al.*, “A new method of filtering T waves to detect hidden P waves in electrocardiogram signals,” *Europace*, vol. 13, no. 7, pp. 1028–1033, 2011.

[12] F. D. Murgatroyd and A. D. Krahn, “Atrial arrhythmias,” in *Handbook of Cardiac Electrophysiology: A Practical Guide Invasive EP Study Catheter Ablation*. London, England: Remedica, 2002, pp. 55–70.

[13] P. Laguna, R. Jané, and P. Caminal, “Automatic detection of wave boundaries in multilead ECG signals: Validation with the CSE database,” *Comput. Biomed. Res.*, vol. 27, no. 1, pp. 45–60, Feb. 1994.

[14] O. Perlman, A. Katz, N. Weissman, and Y. Zigel, “Atrial electrical activity detection in the 12-lead ECG using synthetic atrial activity signals,” in *Proc. Comput. Cardiol.*, Krakow, Poland, 2012, pp. 665–668.

[15] M. S. Link, “Evaluation and initial treatment of supraventricular tachycardia,” *New England J. Med.*, vol. 367, no. 15, pp. 1438–1448, Oct. 2012.

[16] R. O. Bonow, D. L. Mann, D. P. Zipes, and P. Libby, *Braunwald’s Heart Disease: A Textbook of Cardiovascular Medicine*, 8th ed. Amsterdam, The Netherlands: Elsevier, 2007.

[17] S. Nattel, “New ideas about atrial fibrillation 50 years on,” *Nature*, vol. 415, pp. 219–226, 2002.

[18] R. H. Falk, “Atrial fibrillation,” *New England J. Med.*, vol. 344, no. 14, pp. 1067–1078, Apr. 2001.

[19] J. Slocum, A. Sahakian, and S. Swiryn, “Diagnosis of atrial fibrillation from surface electrocardiograms based on computer-detected atrial activity,” *J. Electrocardiol.*, vol. 25, no. 1, pp. 1–8, 1992.

[20] A. K. Jain, R. P. W. Duin, and J. Mao, “Statistical pattern recognition: A review,” *IEEE Trans. Pattern Anal. Mach. Intell.*, vol. 22, no. 1, pp. 4–37, Jan. 2000.

[21] M. G. Tsipouras and D. I. Fotiadis, “Automatic arrhythmia detection based on time and time–frequency analysis of heart rate variability,” *Comput. Methods Programs Biomed.*, vol. 74, no. 2, pp. 95–108, 2004.

[22] T. Cover and P. Hart, “Nearest neighbor pattern classification,” *IEEE. Trans. Inf. Theory*, vol. 13, no. 1, pp. 21–27, Jan. 1967.

[23] A. L. Goldberger *et al.*, “Physiobank, physiotoolkit, and physionet: Components of a new research resource for complex physiologic signals,” *Circulation*, vol. 101, no. 23, pp. e215–e220, Jun. 2000.

[24] A. Jovic and N. Bogunovic, “Evaluating and comparing performance of feature combinations of heart rate variability measures for cardiac rhythm classification,” *Biomed. Signal Process. Control*, vol. 7, pp. 245–255, 2012.

[25] R. G. Newcombe, “Two-sided confidence intervals for the single proportion: Comparison of seven methods,” *Statist. Med.*, vol. 17, no. 8, pp. 857–872, 1998.

[26] A. Jain and D. Zongker, “Feature selection: Evaluation, application, and small sample performance,” *IEEE Trans. Pattern Anal. Mach. Intell.*, vol. 19, no. 2, pp. 153–158, Feb. 1997.

[27] A. K. Jain and B. Chandrasekaran, “Dimensionality and sample size considerations in pattern recognition practice,” in *Handbook of Statistics*, vol. 2, P. R. Krishnaiah and L. N. Kanal, Eds. Amsterdam, The Netherlands: North Holland, 1982, pp. 835–855.

[28] B. K. Kantharia, “P waves in the electrocardiogram recording of tachycardia: ‘You can run, but you cannot hide’,” *Europace*, vol. 13, no. 7, pp. 916–917, 2011.

[29] A. D. Krahn, R. Yee, G. J. Klein, and C. Morillo, “Inappropriate sinus tachycardia: Evaluation and therapy,” *J. Cardiovascular Electrophysiol.*, vol. 6, no. 12, pp. 1124–1128, 1995.

[30] D. Duverney, J. M. Gaspz, V. Pichot, F. Roche, R. Brion, A. Antoniadis, and J. C. Barthelemy, “High accuracy of automatic detection of atrial fibrillation using wavelet transform of heart rate intervals,” *Pacing Clinical Electrophysiol.*, vol. 25, no. 4, pp. 457–462, 2002.

Authors’ photographs and biographies not available at the time of publication.